FAST TRACK COMMUNICATION

Reversible UV induced metal–semiconductor transition in In_2O_3 thin films prepared by autowave oxidation

Fast Track Communications

IOP Publishing Semiconductor Science and Technology

Semicond. Sci. Technol. **29** (2014) 082001 (6pp) doi:10.1088/0268-1242/29/8/082001

Fast Track Communication

Reversible UV induced metal–semiconductor transition in In_2O_3 thin films prepared by autowave oxidation

Igor A Tambasov[1], Victor G Maygkov[1,2], Anton S Tarasov[1], Alexander A Ivanenko[1], Liudmila E Bykova[1], Ivan V Nemtsev[1,3], Evgeny V Eremin[1] and Ekaterina V Yozhikova[2]

[1] Kirensky Institute of Physics, Siberian Branch of the Russian Academy of Sciences, Akademgorodok 50, 660036 Krasnoyarsk, Russia
[2] Reshetnev Siberian State Aerospace University, Krasnoyarsk Worker 31, 660014 Krasnoyarsk, Russia
[3] Krasnoyarsk Scientific Center, Siberian Branch of the Russian Academy of Sciences, Akademgorodok 50, 660036 Krasnoyarsk, Russia

E-mail: tambasov_igor@mail.ru

Received 6 March 2014, revised 18 April 2014
Accepted for publication 16 May 2014
Published 13 June 2014

Abstract

We have prepared thin indium oxide films by the autowave oxidation reaction. Measurements of temperature dependence of resistivity, Hall carrier concentration and Hall mobility have been conducted in the temperature range 5–272 K. Before ultraviolet (UV) irradiation, the indium oxide film had a semiconductor-like temperature dependence of resistivity ρ and the ratio of ρ (5 K)/ρ(272 K) was very limited (∼1.2). It was found that after UV irradiation of the In_2O_3 film, the metal–semiconductor transition (MST) was observed at ∼100 K. To show that this MST is reversible and repeatable, two full cycles of 'absence of MST–presence of MST' have been done using UV irradiation (photoreduction) as the induced mechanism and exposure to an oxygen environment as the reversible mechanism, respectively. MST in transparent conducting oxide (TCO) is possibly associated with the undoped structure of metal oxide, which has some disorder of oxygen vacancies. It was suggested that reversible UV induced metal–semiconductor transition would occur in other TCOs.

Keywords: indium oxide thin films, autowave oxidation, metal-semiconductor transition, UV irradiation, photoreduction

(Some figures may appear in colour only in the online journal)

Transparent conducting oxide (TCO) layers are characteristically described as thin films that exhibit high visible wavelength transparency and electrical conductivity, simultaneously [1]. Two important widely used TCO materials are In_2O_3, and Sn doped In_2O_3 (commonly referred to as ITO) [2–4]. In_2O_3 thin films have been used in gas sensors, transparent thin-film transistors, flat panel displays, electrochromic devices and solar cells [3, 5–10]. The physical-chemical properties of indium oxide thin films strongly depend on the preparation method [3, 11–17]. Currently, inexpensive methods that allow synthesizing the In_2O_3 films at low temperatures are being developed [8, 11, 13, 18, 19]. Among these methods, a process of metal oxide film deposition using a combustion mode has been proposed for temperatures below 200 °C [11]. Recently, we investigated In_2O_3 thin films, which were produced by autowave oxidation with a low initiation temperature (180 °C) [20]. Autowave oxidation is a promising method for obtaining the indium oxide thin film because it is inexpensive, simple and has a relatively low temperature of synthesis. The autowave oxidation nature in

the thin films was similar to the self-propagating high-temperature synthesis (SHS) method for powders, which is now widely used for the production of new materials [21]. SHS products are high-quality compounds and are believed to contain fewer impurities than the original mixtures [21]. SHS can be performed in a wide range of materials including fine powders, liquids, gases and thin TCO films [11, 22, 23].

It has recently become known that some TCO thin films can have interesting physical phenomena such as metal–semiconductors (MSTs) or sometimes noted as metal–insulator transitions (MITs) in publications [24–33]. MSTs or MITs in metal oxide and other semiconductors are objects of scientific interest [28, 34]. These transitions occur at a wide temperature range [28] and are observed in doped TCO thin films [24–33]. However, recent reports have been presented that show such transitions can occur in undoped TCO, such as In_2O_3 [35] and ZnO [36–38] at low temperatures. It should be noted that undoped TCO films, which have MST, were prepared at certain substrate temperatures. At other substrate temperatures, MST has not been observed [35, 37] at low temperatures. Furthermore, MST can be induced in ZnO by the introduction of H_2 in a vacuum chamber at sputtering thin films [39]. MST can be explained using a model proposed for conduction in disordered matter [40]. In fact, thin epitaxial In_2O_3 films, which had a part of a disordered phase, have shown MST [35]. Moreover, oxygen vacancies do play a major role on the electrical properties in TCO. Thus, understanding the oxygen vacancies influences in MST or MIT is the actual problem.

Oxygen vacancy concentration in TCO can be increased or reduced by ultraviolet (UV) irradiation (called photoreduction) or exposure to an oxygen environment, respectively [41, 42]. These two manipulation mechanisms in TCO are opposites of each other. Photoreduction is a very useful mechanism for gas sensing because the sensor operating temperature can be decreased. Ultraviolet irradiation has been shown to affect the resistivity of indium oxide films [41, 43–46]. As a result of UV irradiation, the indium oxide films showed a sharp decrease in resistivity. After UV irradiation, the resistivity was slowly restored. The quantitative change in the resistivity of the In_2O_3 films irradiated with UV light was strongly dependent on the film's structure and morphology [43, 45, 46]. This effect could be used to improve the sensitivity of gas sensors based on indium oxide thin films [42, 44, 46, 47]. However, we have not found investigations related to the study of the UV influences on MST or MST in TCO. Only one mention was found in [48]. In [48] it was shown that after UV irradiation, thin SnO_2 films had metal and semiconductor-like type of temperature dependence of resistivity. But, there are no detailed transport properties or an accented explanation of the effect.

Here we present a new observed phenomenon, which is the reversible UV induced metal-semiconductor transition that occurs at low temperatures in In_2O_3 thin films. This phenomenon is implemented using photoreduction as the induced mechanism and exposure to an oxygen environment as the reversible mechanism, respectively. The measurements of temperature dependence of resistivity, Hall carrier concentration and Hall mobility are presented.

Indium oxide films were prepared by the autowave oxidation reaction [20]. The initial $In + In_2O_3$ films were obtained by thermal evaporation of pure indium (99.999%) at a pressure of 1.5 Torr. The films were deposited on cover glass and quartz substrates at room temperature. Prior to deposition, the substrates were cleaned in an ultrasonic bath with acetone and then methanol. Autowave oxidation reactions were carried out by heating the initial $In + In_2O_3$ films with a speed of $>1\ K\ s^{-1}$, to a temperature of 200 °C at a pressure of 0.5 Torr. After reaching the initiation temperature, $T_0 \approx 180$ °C, the nucleation of the In_2O_3 phase began, spreading over the surface in a self-sustaining manner [20]. It has been shown that after the autowave oxidation, thin In_2O_3 films had a homogenous surface with crystallite size of 20–40 nm. The ratio of In/O was also homogenous on the film thickness and was ≈1.12. X-ray diffraction has revealed that the thin film had only bixbyite crustal structure of In_2O_3 [20].

The film thickness was measured using a Hitachi S5500 scanning electron microscope in cross-section and was approximately 300 nm. A Hg discharge lamp was used as the UV source and a 3.1–5.0 eV bandpass filter was applied to obtain the UV wavelengths from the lamp's emission spectrum. The lamp emission power was about 0.1 W on the film surface. To estimate the optical band gap of the films a Shimadzu UV-3600 spectrophotometer was used.

The transport properties were investigated from 5 to 272 K using a standard four-probe method. Pt contacts on top of thin In_2O_3 film were used and sputtered using an Emitech k575x sputter coater. The thickness of the Pt contacts was approximately 80 nm. The temperature dependence measurements of the resistivity, Hall carrier concentration and Hall mobility of the In_2O_3 sample were performed using an original facility based on a helium cryostat, an electromagnet, and a precise Keithley-2400 current/voltage source meter [49]. There is a quartz window in this helium cryostat. To input UV irradiation into this helium cryostat we placed the Hg discharge lamp in front of the quartz window. The transport properties were measured in a dc mode at a fixed value of the current and at a magnetic field of 6 kOe. The electronic properties of thin In_2O_3 film was studied for four cases processing which are quoted in table 1 and named Step1, Step2, Step3 and Step4. These four steps correspond to two full cycles of the 'absence of MST–presence of MST' scheme to demonstrate reversibility and repeatability of this phenomenon.

From the transmittance data, the absorption coefficient squared (α^2) was calculated as a function of the photon energy $h\nu$ (plotted in figure 1) for the allowed transitions by using the Tauc model and parabolic bands [50]: $(\alpha h\nu)^2 = A(h\nu - E_g)$, where A is a proportionality constant and E_g is the optical band gap. The value of the optical band gap was obtained by extrapolating the tangential line of the data to the abscissa axis, where $(\alpha h\nu)^2$ was plotted as a function of $h\nu$, shown in figure 1. The optical band gap for the as-deposited In_2O_3 thin film was estimated to be 3.5 eV. This value agrees well with other experimental values for indium oxide films

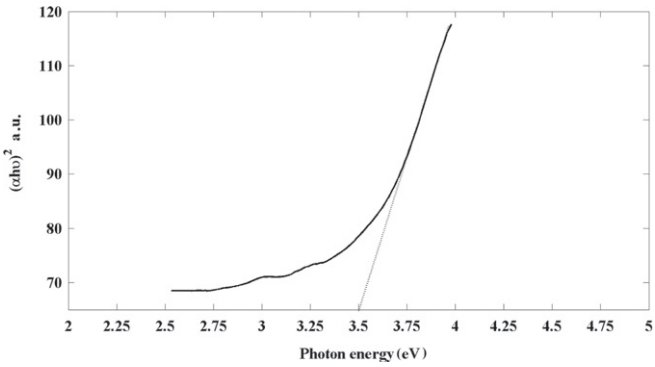

Figure 1. Square of absorption coefficient $(\alpha h\nu)^2$ as a function of photon energy for an In_2O_3 thin film on a quartz substrate.

Table 1. Sequential processing of thin In_2O_3 film.

Name processing	Processing	Processing time (hours)
Step1	As-deposited	—
Step2	UV irradiation	3
Step3	Exposing in air	24
Step4	UV irradiation	3

[27, 35, 51, 52]. For the photoreduction effect it is necessary that energy irradiation must be larger than the optical band gap [42]. Thus, in our case photoreduction will take place. On the other hand, we have not observed the change of the value of the optical band gap after UV irradiation.

Figure 2 shows the dependence of the indium oxide film resistivity (ρ) versus temperature in the range 3–272 K, measured in the dark for four processing. The ratio of ρ(5 K)/ρ(272 K) for as-deposited thin In_2O_3 film is very limited (1.2) as shows in figure 2(a). Indeed, for classical semiconductors (thermally activated conduction) this value is always higher than 20. However, similar behavior of thin indium oxide film resistivity has been observed and reported recently in [35]. In addition, similar behaviors of resistivity were observed for other metal oxides [28, 38]. After UV irradiation as shown in figure 2(b), MST is observed. The ratios of $\rho(5\,K)_{Step1}/\rho(5\,K)_{Step2}$ and $\rho(272\,K)_{Step1}/\rho(272\,K)_{Step2}$ are 2.725 and 2.015, respectively. To test reversibility and reproducibility of this phenomenon we conducted appropriate processing Step3 and Step4 (figures 2(c)–(d)). It is clearly seen from figure 2 that observed MST in thin In_2O_3 films can be induced and suppressed by UV irradiation and exposing in air, respectively. In addition, the ratios of $\rho(5\,K)_{Step3}/\rho(5\,K)_{Step4}$ and $\rho(272\,K)_{Step3}/\rho(272\,K)_{Step4}$ are 2.849 and 2.112 which are close to the values for Step1 and Step2. The transition temperatures T_{MST} (figures 2(b) and (d)) are 105 K and 97 K. These values of T_{MST} are close to the transition temperature for thin undoped indium oxide films ($T_{MST} = 118$ K [35]). Moreover, T_{MST} of Sn doped In_2O_3 were 94 K [31], 87 K [26], approximately 100 K and 80 K [25]. For Nb doped In_2O_3 T_{MST} was ~100 K [53]. From these data, we suggest that a feature of the undoped structure of indium oxide should be mainly responsible for MST. This feature of the structure should consist in the location and concentration of oxygen vacancies in indium oxide. To date, there are publications for TCO based on ZnO, where MST has been observed. To extend our hypothesis we have collected data on T_{MST} from these publications. T_{MST} for undoped ZnO were ~160 K [37], ~150 K [36] and ~195 K [36]. T_{MST} for H doped ZnO were 165 K and 210 K [39]. In addition, TMS has been reported in Ga doped ZnO at 160 K [33], 170 K [54], 141 K [24]. Al and Er doped ZnO had TMS at 150 K [55] and 190 K [56], respectively. The degree of disorder leads to a shift of the transition temperature in undoped thin ZnO films [36]. Thus, MST in TCO should be linked mainly with the undoped structure of metal oxide, which has a specific structural disorder of oxygen vacancies.

The temperature dependent resistivity of TCO is often explained by Mott's variable-range hopping [35, 39]. The critical carrier concentration for the onset of metallic resistivity as given by the Mott criterion is estimated to be 7.2×10^{18} cm^{-3} for In_2O_3 [57]. From figure 3(a) it can be seen that the carrier concentrations (n) are above the Mott concentration. A model proposed for conduction in disordered matter [40] can be used when the required condition Fermi wavelength $\lambda_F = \left(\frac{2\pi}{(3\pi^2 n)^{1/3}}\right)$ is comparable to the electronic mean free path $\Lambda = \left(\frac{h}{\rho n e^2 \lambda_F}\right)$. For Step2 and Step4, we obtained λ_F (8.65 nm, 6.615 nm) > Λ (0.943 nm, 0.582 nm) at transition temperatures of 105 K and 97 K, hence, quantum corrections (QCs) could be taken into account to interpret the transport mechanisms as given by the following equation [40]:

$$\rho = \frac{1}{\sigma_0 + aT^{p/2} + mT^{1/2}} + bT^2, \qquad (1)$$

where σ_0 is related to residual conductivity. These QCs corresponding to weak localization (2nd term in denominator) and Coulomb interaction (the 3rd term in denominator) have been applied in the present work to analyze the resistivity of In_2O_3 film. The corrections are valid provided that their contributions are much smaller than the Boltzmann conductivity. In the present case, this condition is satisfied. The corresponding values of the fitting parameters are given in table 2.

The best fit (solid lines) was obtained for $p = 3$ which means that electron-phonon scattering plays a dominating role in the carrier transport mechanism. The values of a were much smaller compared to m, which established that the contribution of QC to conductivity comes largely from the Coulomb electron interaction [40].

The dependence of the Hall carrier concentration and the Hall mobility (μ) of indium oxide film versus temperature are presented in figure 3. As-deposited, indium oxide film had $\rho = 0.0561\,\Omega$ cm, $n = 5.7 \cdot 10^{19}$ cm^{-3} and $\mu = 1.94$ cm^2 Vs^{-1} at room temperature.

The carrier concentration measured for Step1 increasingly depends on temperature as compared with Step2. Nevertheless, the absolute value of the concentration for Step1 is higher than for Step2. On the other hand, the

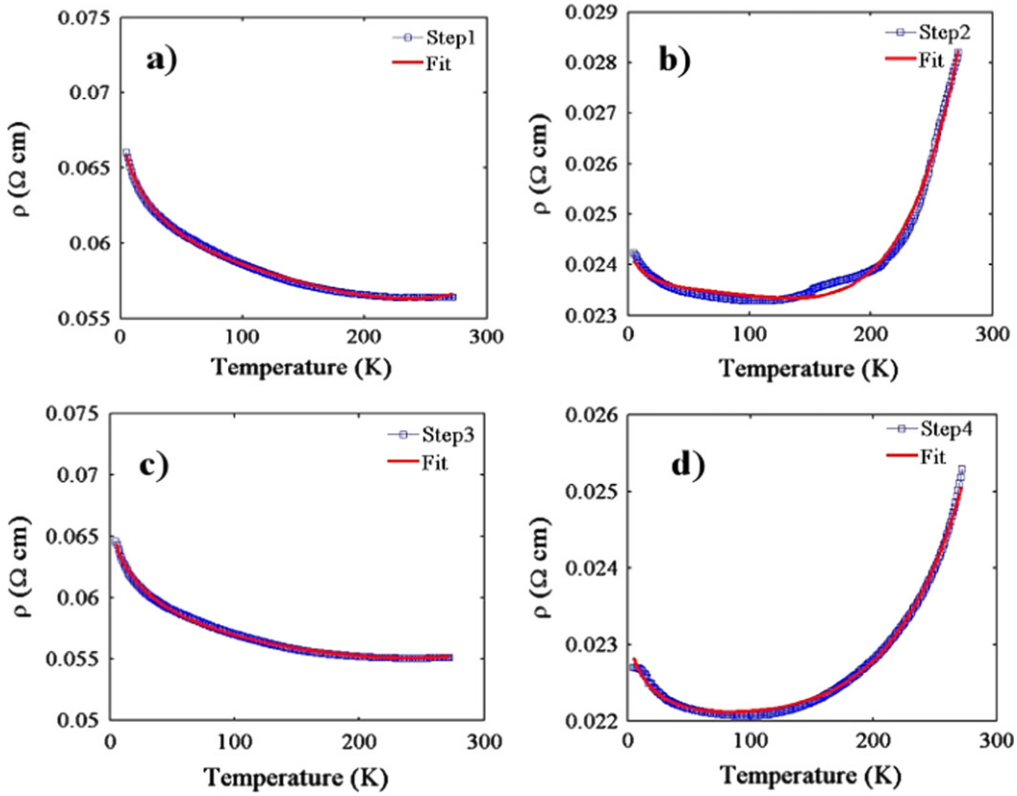

Figure 2. Resistivity as a function of temperature for an In_2O_3 film, measured in the dark for four processing: (a) Step1, (b) Step2, (c) Step3 and (d) Step4. The open squares are experimental data and the red solid line in (a)–(b) is a fit using equation (1).

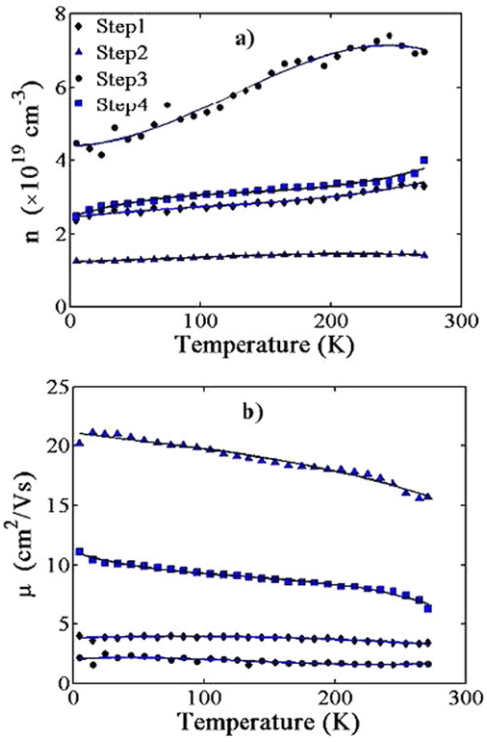

Figure 3. Hall carrier concentration (a) and Hall mobility (b) as a function of temperature for an In_2O_3 film, measured in the dark for four processing. The closed rhombs, triangles, circles and squares are experimental data (the solid lines are an eye guideline).

corresponding carrier mobility for Step1 relatively weakly depends on the temperature as compared with Step2. Moreover, the Step2 mobility value is greater than the mobility value of Step1. A similar situation occurs for Step3 and Step4. The carrier concentration and mobility of Step2 and Step4 could not clearly show MST at ~100 K'.

We assume that MST in TCO is possibly associated with the undoped structure of metal oxide, which has some disorder of oxygen vacancies. However, experimental confirmations are necessary for our hypothesis. It is possible that UV irradiation changes the degree of disorder through a photoreduction effect that leads to MST at low temperatures. However, exposure in air leads to the return to the initial the degree of disorder in In_2O_3 films. We also believe that a reversible UV induced metal–semiconductor transition would occur in other TCO which have semiconductor-like type of resistivity and the limited ratio of $\rho(\sim 5)/\rho(\sim 272\ \mathrm{K})$ (~1). The existences of MSTs in unirradiated In_2O_3 films at high temperatures and UV influence on optical properties are the subject of future study.

In conclusion, we have prepared thin indium oxide films by the autowave oxidation reaction. The measurements of temperature dependence of resistivity, Hall carrier concentration and Hall mobility have been conducted in the temperature range 5–272 K. It was found that after UV irradiation of the In_2O_3 film, MST was observed at ~100 K. We have shown that this phenomenon is reversible by exposure in air and is repeatable. MST in TCO is possibly associated with the undoped structure of metal oxide, which has some

Table 2. Values of the fitting parameters of equation (1) for thin In_2O_3 film at Steps1–4.

Name of Step	σ_0 (Ω^{-1} cm^{-1})	m (Ω^{-1} c m^{-1} K$^{-1/2}$)	a (Ω^{-1} c m^{-1} K$^{-3/2}$)	b (Ω cm K^{-2})
Step1	14.43	0.3465	–0.001545	-2.572×10^{-7}
Step2	39.45	0.6352	–0.005856	-1.88×10^{-7}
Step3	14.72	0.3657	–0.001323	-1.657×10^{-7}
Step4	42.8	0.4778	–0.004805	-1.255×10^{-7}

disorder of oxygen vacancies. It was suggested that a reversible UV induced metal–semiconductor transition would occur in other TCO.

Acknowledgments

This work was supported by the Federal Target Program through Contract № 14.513.11.0023; the Russian Foundation for Basic Research, Project No. 14-02-31156.

References

[1] Calnan S and Tiwari A N 2010 *Thin Solid Films* **518** 1839–49
[2] Karazhanov S Z, Ravindran P, Vajeeston P, Ulyashin A, Finstad T G and Fjellvag H 2007 *Phys. Rev.* B **76** 075129
[3] Granqvist C G 2007 *Sol. Energy Mater. Sol. Cells* **91** 1529–98
[4] King P D C and Veal T D 2011 *J. Phys.: Condens. Matter.* **23** 334214
[5] Han S Y, Herman G S and Chang C H 2011 *J. Amer. Chem. Soc.* **133** 5166–9
[6] Katsarakis N 2004 *J. Phys.: Condens. Matter.* **16** S3757
[7] Jeong S and Moon J 2012 *J. Mater. Chem.* **22** 1243–50
[8] Wang L, Yoon M H, Lu G, Yang Y, Facchetti A and Marks T J 2006 *Nat. Mater.* **5** 893–900
[9] Fortunato E, Barquinha P and Martins R 2012 *Advan. Mater.* **24** 2945–86
[10] Wagner T, Haffer S, Weinberger C, Klaus D and Tiemann M 2013 *Chem. Soc. Rev.* **42** 4036–53
[11] Kim M G, Kanatzidis M G, Facchetti A and Marks T J 2011 *Nat. Mater.* **10** 382–8
[12] Pasquarelli R M, Ginley D S and O'Hayre R 2011 *Chem. Soc. Rev.* **40** 5406–41
[13] Kim M G, Hennek J W, Kim H S, Kanatzidis M G, Facchetti A and Marks T J 2012 *J. Amer. Chem. Soc.* **134** 11583–93
[14] Adurodija F O, Izumi H, Ishihara T, Yoshioka H, Matsui H and Motoyama M 1999 *Appl. Phys. Lett.* **74** 3059–61
[15] Bloor L G, Carmalt C J and Pugh D 2011 *Coordin. Chem. Rev.* **255** 1293–318
[16] Klein A, Korber C, Wachau A, Sauberlich F, Gassenbauer Y, Schafranek R, Harvey S P and Mason T O 2009 *Thin Solid Films* **518** 1197–203
[17] Himmerlich M, Wang C Y, Cimalla V, Ambacher O and Krischok S 2012 *J. Appl. Phys.* **111** 093704
[18] Kim Y H, Heo J S, Kim T H, Park S, Yoon M H, Kim J, Oh M S, Yi G R, Noh Y Y and Park S K 2012 *Nature* **489** 128–32
[19] Sierros K A, Cairns D R, Abell J S and Kukureka S N 2010 *Thin Solid Films* **518** 2623–7
[20] Tambasov I A *et al* 2013 *Semiconductors* **47** 569–73
[21] Merzhanov A G 2003 *Uspekhi Khimii* **72** 323–45
[22] Rajeshwar K and de Tacconi N R 2009 *Chem. Soc. Rev.* **38** 1984–98
[23] Rim Y S, Lim H S and Kim H J 2013 *Acs Appl. Mater. Interf.* **5** 3565–71
[24] Naidu R V M, Subrahmanyam A, Verger A, Jain M K, Rao S V N B, Jha S N and Phase D M 2012 *Electr. Mater. Lett.* **8** 457–62
[25] Liu X D, Jiang E Y and Zhang D X 2008 *J. Appl. Phys.* **104** 073711
[26] Chiquito A J, Lanfredi A J C and Leite E R 2008 *Phys. E: Low Dimen. Syst. Nanostr.* **40** 449–51
[27] Lozano O *et al* 2013 *Sol. Energ. Mater. Sol. Cel.* **113** 171–8
[28] Nistor M and Perriere J 2013 *Sol. Stat. Comm.* **163** 60–4
[29] Gao K H *et al* 2013 *Sol. Stat. Comm.* **157** 49–53
[30] Sun J, Yang W, Huang Y, Lai W S, Lee A Y S, Wang C F and Gong H 2012 *J. Appl. Phys.* **112** 083709
[31] Guo E-J, Guo H, Lu H, Jin K, He M and Yang G 2011 *Appl. Phys. Lett.* **98** 011905
[32] Lin B-T, Chen Y-F, Lin J-J and Wu C-Y 2010 *Thin Solid Films* **518** 6997–7001
[33] Li Y, Huang Q and Bi X 2013 *J. Appl. Phys.* **113** 053702
[34] Siegrist T, Jost P, Volker H, Woda M, Merkelbach P, Schlockermann C and Wuttig M 2011 *Nat. Mater.* **10** 202–8
[35] Seiler W, Nistor M, Hebert C and Perriere J 2013 *Sol. Energ. Mater. Sol. Cel.* **116** 34–42
[36] Saha D, Das A K, Ajimsha R S, Misra P and Kukreja L M 2013 *J. Appl. Phys.* **114** 043703
[37] Nistor M, Gherendi F, Mandache N B, Hebert C, Perriere J and Seiler W 2009 *J. Appl. Phys.* **106** 103710
[38] Nistor M, Mandache N B, Perriere J, Hebert C, Gherendi F and Seiler W 2011 *Thin Solid Films* **519** 3959–64
[39] Singh A, Chaudhary S and Pandya D K 2013 *Appl. Phys. Lett.* **102** 172106
[40] Lee P A and Ramakrishnan T V 1985 *Rev. Mod. Phys.* **57** 287–337
[41] Bender M, Katsarakis N, Gagaoudakis E, Hourdakis E, Douloufakis E, Cimalla V and Kiriakidis G 2001 *J. Appl. Phys.* **90** 5382–7
[42] Wagner T, Kohl C D, Morandi S, Malagu C, Donato N, Latino M, Neri G and Tiemann M 2012 *Chem. Europ. J.* **18** 8216–23
[43] Qin L, Dutta P S and Sawyer S 2012 *Semicond. Sci. Technol.* **27** 045005
[44] Wang C Y, Cimalla V, Kups T, Rohlig c.c., Romanus H, Lebedev V, Pezoldt J, Stauden T and Ambacher O 2007 *J. Appl. Phys.* **102** 044310
[45] Olivier J, Servet B, Vergnolle M, Mosca M and Garry G 2001 *Synth. Met.* **122** 87–9
[46] Kiriakidis G, Moschovis K, Kortidis I and Binas V 2012 *Vacuum* **86** 495–506
[47] Wagner T, Hennemann J, Kohl C D and Tiemann M 2011 *Thin Solid Films* **520** 918–21
[48] Muraoka Y, Takubo N and Hiroi Z 2009 *J. Appl. Phys.* **105** 103702
[49] Volkov N V, Tarasov A S, Eremin E V, Baron F A, Varnakov S N and Ovchinnikov S G 2013 *J. Appl. Phys.* **114** 093903
[50] Cho S 2012 *Microelectron. Eng.* **89** 84–8
[51] Tripathi N, Rath S, Ganesan V and Choudhary R J 2010 *Appl. Surf. Scien.* **256** 7091–5

[52] Chopra K L, Major S and Pandya D K 1983 *Thin Solid Films* **102** 1–46
[53] Lozano O *et al* 2013 *Sol. Energ. Mater. Sol. Cell* **113** 171–8
[54] Bhosle V, Tiwari A and Narayan J 2006 *Appl. Phys. Lett.* **88** 032106
[55] Bamiduro O, Mustafa H, Mundle R, Konda R B and Pradhan A K 2007 *Appl. Phys. Lett.* **90** 252108
[56] Pradhan A K, Douglas L, Mustafa H, Mundle R, Hunter D and Bonner C E 2007 *Appl. Phys. Lett.* **90** 072108
[57] Zhang K H L *et al* 2009 *Chem. Mater.* **21** 4353–5